AVS Quantum Science

RESEARCH ARTICLE | SEPTEMBER 28 2023

Suppressing communication errors using quantum-enabled forward error correction

Ivan A. Burenkov ; N. Fajar R. Annafianto; M. V. Jabir ; Abdella Battou ; Sergey V. Polyakov

AVS Quantum Sci. 5, 031403 (2023)
https://doi.org/10.1116/5.0164396

AVS
AIP Publishing

Suppressing communication errors using quantum-enabled forward error correction

Cite as: AVS Quantum Sci. 5, 031403 (2023); doi: 10.1116/5.0164396
Submitted: 22 June 2023 · Accepted: 5 September 2023 ·
Published Online: 28 September 2023

Ivan A. Burenkov,[1,2,a)] N. Fajar R. Annafianto,[2] M. V. Jabir,[2] Abdella Battou,[2] and Sergey V. Polyakov[2,3]

AFFILIATIONS

[1]Joint Quantum Institute, University of Maryland, College Park, Maryland 20742, USA
[2]National Institute of Standards and Technology, Gaithersburg, Maryland 20899, USA
[3]Physics Department, University of Maryland, College Park, Maryland 20742, USA

[a)]Electronic mail: ivan.burenkov@gmail.com

ABSTRACT

Because noise is inherent to all measurements, optical communication requires error identification and correction to protect and recover user data. Yet, error correction, routinely used in classical receivers, has not been applied to receivers that take advantage of quantum measurement. Here, we show how information uniquely available in a quantum measurement can be employed for efficient error correction. Our quantum-enabled forward error correction protocol operates on quadrature phase shift keying (QPSK) and achieves more than 80 dB error suppression compared to the raw symbol error rate and approximately 40 dB improvement of symbol error rates beyond the QPSK classical limit. With a symbol error rate below 10^{-9} for just 11 photons per bit, this approach enables reliable use of quantum receivers for ultra-low power optical communications. Limiting optical power improves the information capacity of optical links and enables scalable networks with coexisting quantum and classical channels in the same optical fiber.

I. INTRODUCTION

The exchange of physical states and their measurement are required for any communication. The trade-off between the amount of physical resources used and the chance of erroneous transmission is fundamental, owing to the nature of measurement. In the absence of error correction mechanisms, reliable communication requires significant energy and bandwidth use. A quantum measurement can reduce the symbol error rate (SER) beyond what is possible with classical state identification, particularly when faint states of light are used for communication.[1] The SER is commonly defined as a ratio of the number of state identification measurement outcomes resulting in the wrong state (symbol) to the total number of states (symbols) transmitted to the receiver. Here, we show that error correction also can be enhanced by taking advantage of quantum measurement.

A significant research effort in quantum-enhanced communications is ongoing, and experimental results demonstrate error rate suppression below the classical shot-noise limit (SNL). These experiments[2–12] achieved below the SNL symbol error rates with the optical signal energy of just ≈ one photon per bit at the receiver. This result is impressive from a fundamental point of view. Yet, error rates at this input energy are too high for practical use even with the quantum enhancement. One of the ways to reduce the error rate is to increase the power of the optical carrier. Unfortunately, higher power often results in saturation of quantum receivers due to experimental deficiencies such as imperfect displacement to a vacuum state. We are aware of one experiment that extended symbol error rates below the SNL for input signals with energies of up to ten photons per bit. In that work, a raw symbol error rate of $\approx 3 \times 10^{-7}$ was achieved using a photon-number resolving receiver,[13] but there is still a significant gap between the demonstrated SER and the fundamental quantum bound.

In this work, we implement a different approach: we combine multiple symbols, each containing just one photon per bit, into a codeword. In our recent work,[14] we introduced the concept of confidence *a posteriori* probabilities (CAPPs) and identified their fundamental properties. Here, we expand forward error correction (FEC), an inseparable part of classical communication,[15] for quantum receivers and experimentally demonstrate that CAPPs improve the performance of forward error correction codes. To take advantage of the continuous quantum measurement, we analyze properties of CAPPs beyond.[14,16] Multiple different quantum-enabled forward error correction (QEFEC) codes were tested, and underperforming ones were rejected.

We report on error-correcting protocols with the best SER scaling with symbol energy to our knowledge. To this point, our protocols yield a record low symbol error rate of 10^{-9}, approximately 40 dB below the quadrature phase shift keying (QPSK) classical error limit for 11 photons per bit at the receiver. Interestingly, the use of quantum-enabled FECs yields better results with quantum receivers than merely increasing the input energy.[13]

II. METHODS

Consider a single-shot state identification where only a single copy of the input state is available. In this experiment, we employ quadrature phase shift keying (QPSK), where each symbol encodes $\log_2 4 = 2$ bits. The QPSK alphabet consists of four coherent states $|\alpha_m\rangle$ with the same mean photon number $n = |\alpha|^2 = |\alpha_m|^2$, and complex parameter $\alpha_m = |\alpha| e^{im\pi/2}$, where $m \in \{0, 1, 2, 3\}$. Symbols are encoded as flat-top laser pulses.

Usually, state identification measurement is comprised of interfering the input signal with a local oscillator (LO) and detecting the resulting signal (homodyne or heterodyne detection). In contrast, in experimental implementations of quantum receivers, the adaptive LO is used.[5,6,8–10,12,13,16,17] The quantum receiver,[8,16] which we developed and utilized for experimental measurements, continuously measures photon detection times and updates the local oscillator state upon photon detection. Continuous measurement for photon counting was introduced in Ref. 18. The theory of the continuous measurement used in this manuscript is published in Ref. 14. The continuous measurement yields a continuum of outcomes—CAPPs for each symbol. The measurement record that contains displacements applied at each time and timestamps of each photon detection is obtained, and the corresponding Bayesian probabilities are computed for each possible input state. All components of the CAPP vector will be used by our error-correcting algorithms.

In our quantum receiver, an adaptive algorithm finds the LO that displaces an input state to vacuum (produces destructive interference), and a single-photon detector verifies the displacement. Ideally, if the LO matches the input, no photons reach the detector. Otherwise, the displacement at the beam splitter will result in a higher probability to detect photons at the output. The detection of a photon indicates that the LO and the input are not matched. Therefore, the longer no photons are detected, the higher the chance that the LO matches the input signal, which can be expressed as a Bayesian probability. If a photon is detected, most probably the current LO did not match the input, so the new LO is identified. We employ Bayesian inference to identify the most likely state and calculate the likelihood of each communication alphabet symbol using the measurement record consisting of the history of previously applied LOs and photon detection times[8,16] (also see the video description of the algorithm[19]). Then the new LO is switched to the new most likely input state. At the end of the signal pulse, CAPPs are the set of *a posteriori* Bayesian probabilities inferred from the adaptive measurement. An example of one identification measurement is shown in the inset of Fig. 1 to illustrate the algorithm and it includes a measurement record and corresponding CAPPs. In the naive use of CAPPs, only the state with the highest probability is used as a state identification outcome. We have shown[14] that these probabilities give more complete information about the measurement. In this work, we show that the information contained in CAPPs can be efficiently used for quantum-enabled error correction.

Figure 1 identifies relevant blocks of the time-resolving quantum receiver experimental testbed; the complete experimental setup can be found in Refs. 8 and 20. The field-programmable gate array (FPGA) generates RF pulses at ≈80 MHz to prepare the optical states for both signal and LO arms of the testbed, runs the quantum state identification algorithm, and computes CAPP values for each received symbol. The quantum state identification is based on a displacement of the input optical signal that occurs on a $\mathscr{R} : \mathscr{T} \approx 1 : 99$ fiber beam splitter (FBS). The displaced state is measured with a single-photon detector, here a commercial superconducting nanowire single-photon detector (SNSPD) with high detection efficiency and low dark count rate operating at 800 mK.

The measured mean photon number of the input state is two photons/pulse, and the LO is ≈100 times stronger than the input state before the beam splitter. The symbol duration is $T = 64.4\,\mu$s; however, we further normalize it to a unit length $T = 1$ because the actual duration of the signal pulse is not relevant to the results of this work. The measured visibility of the interferometer is 99.4%. The system efficiency is 88.5(5)%, which includes propagation loss of 7.5(2)% and detection efficiency of 95.7(5)%, where the uncertainties are mainly due to the statistical uncertainty of calibrating the attenuators (see Ref. 20 for details).

To simplify the testbed, we use the same personal computer (PC) and field-programmable gate array (FPGA) to encode, send, receive, and analyze the user-defined data. To develop and test error correction protocols, we experimentally prepare, send, and receive a data sequence that contains more than 10^8 symbols. We ensure that each of the four possible states of the QPSK alphabet is used an equal number of times in the data sequence to ensure that all the QPSK states are equiprobable. We collect experimental data for this sequence, which consists of state identifications (successful and unsuccessful) and associated CAPPs. To test quantum-enabled forward error correction protocols, we generate all valid codewords using symbols obtained in the experiment (i.e., with state identification errors due to measurement) in a cycle. Then we calculate the SER of the QEFEC protocol as the number of errors in transmitted information symbols not corrected by the FEC protocol divided by the total number of information symbols encoded in codewords used in the protocol test. For this last step, we find the number of errors by comparing the sent and received datasets after codewords are decoded.

III. RESULTS

In the case of the M-PSK modulation, the SNL takes a simple analytical form[21] as a function of average number of photons n,

$$P_{\text{error}}^{\text{SNL}}(n) = 1 - \frac{1}{\pi}\int_0^{\infty}\int_{-\pi/M}^{\pi/M} e^{-|re^{i\theta}-\sqrt{n}|^2} r dr d\theta,$$

where $M = 4$ for QPSK. In our experiments, we obtain below the shot-noise limit symbol error rates[8–10] with the input energy of just ≈ one photon per bit. The raw experimental SER at that input energy is about 8%, i.e., below the classical SNL.

Here, we take advantage of additional information about the input state available through a continuous quantum measurement to develop and test a practical error correction protocol. Particularly, we combine multiple symbols into codewords and use the CAPPs obtained for each symbol[14] to correct communication errors. The idea of supplementing FEC with CAPPs is agnostic to a modulation

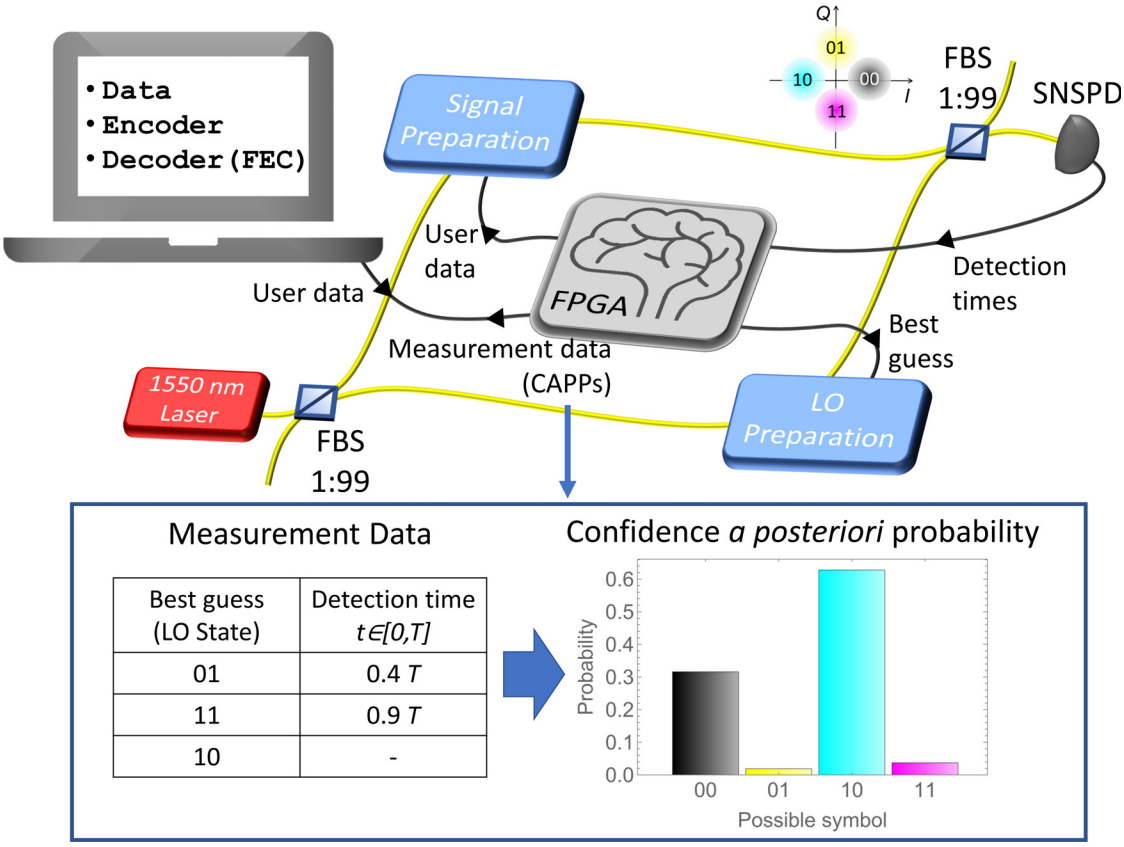

FIG. 1. Schematic of the quantum receiver testbed. The LO is combined with the signal on a 1:99 fiber beam splitter (FBS) that is almost transparent for the signal light. If the LO is in the same state as the input, it will displace the signal to the vacuum state. A superconducting nanowire single-photon detector (SNSPD) is used to detect photons. Data can be encoded and transferred to a field-programmable gate array (FPGA). The FPGA controls a signal preparation module that encodes information by modulating the laser light. The same FPGA receives and processes information from single-photon detections and controls a local oscillator (LO). The FPGA retains measurement records and computes CAPPs for each input symbol. These data are transferred to a PC and used to develop and test forward error correction (FEC) strategies. Inset: Example of a measurement record and corresponding CAPPs for a case of communication alphabet consisting of four symbols. In this example, the receiver first probes state "01." The LO state is only changed when a photon is detected. The first photon is detected at the time $t = 0.4T$, the receiver switches LO to the next state "11." At $t = 0.9T$, the second photon is detected, and the receiver switches to the next state "10." No more photons are detected. Only two detections have occurred; therefore, only three out of four states were tested. Particularly, the state "00" was never tested. Because the state "10" was only tested for a short period of time (1/10 of the total pulse duration T) and no photons were detected, the receiver did not have enough time to distinguish the "10" state from the "00" state with high confidence. In contrast, testing states "11" and "01" resulted in photon detection, making these states highly unlikely. Thus, both states "00" and "10" have high *a posteriori* probabilities (confidences) at the end of the measurement.

scheme and can be applied to any practical quantum state identification method.

A. Direct demonstration of quantum measurement advantage using repetition error correction code

First, we intend to demonstrate that CAPP data available for each measurement enhance error correction. Indeed, it was shown that CAPP values that are single-measurement-based estimates of Bayesian probabilities are in good agreement with ensemble-averaged Kolmogorov probabilities.[14] As such, CAPPs contain useful information about how trustworthy each individual measurement outcome is. To demonstrate such an advantage directly, we analyze the simplest repetition code[15] with and without the use of CAPP data. As follows from its name, the repetition code repeats an information symbol; each copy of the symbol is received separately. If the correct received symbol is identified by simple voting, a decoding error often occurs because the reliability of each symbol identification is not considered. Here, we show that decoding errors can be reduced by supplementing each measurement outcome with the CAPP vector obtained from the quantum measurement. Indeed, by comparing products of confidences for all possible measurement outcomes significantly more errors can be corrected. We use an example of a binary alphabet for the simplicity of the concept illustration. We consider a hypothetical outcome of the repetition code where the same symbol was sent five times. In Fig. 2, we show a typical scenario where a simple voting strategy leads to an error. In contrast, the inclusion of CAPP information, a continuous output of the otherwise discrete state identification problem, correctly identifies a transmitted state for the same hypothetical measurement outcomes.

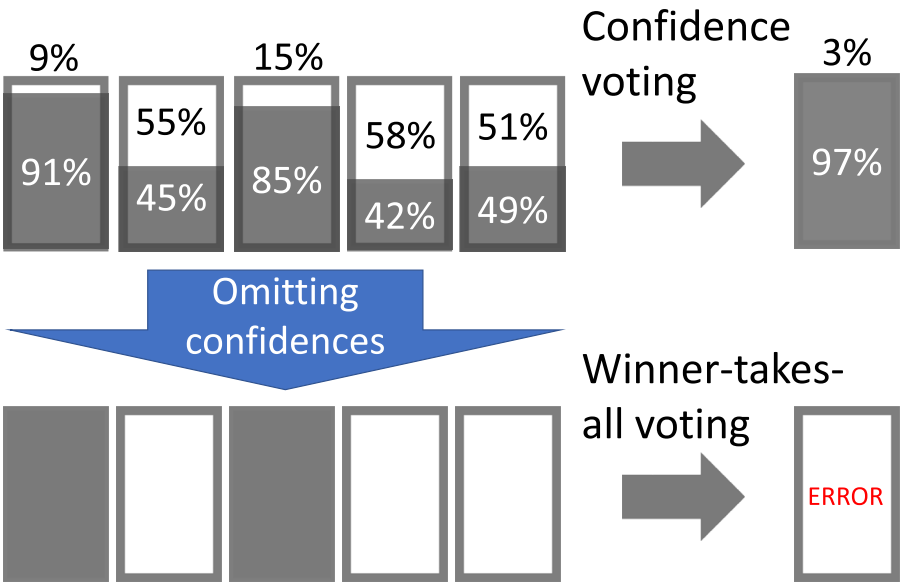

Fig. 2. Comparison of the confidence voting strategy and the simple voting strategy for the repetition FEC code. A hypothetical binary alphabet (gray or white) is used for simplicity, and the gray state was sent. In this case, quantum measurement yields two CAPP values for each received symbol. The confidence voting relies on the estimated probability to obtain each of the possible codewords using CAPP data. Then the cumulative estimated probability for the codeword yields the gray state with 97 % confidence. In a simple voting strategy, only the measurement outcome with the highest confidence is preserved after each state identification. Because confidence information is ignored, the winner state is selected by plurality. The outcomes considered here show that preserving confidences for each transmitted symbol allows one to correct an error, while simple plurality voting leads to the decoding error.

In Fig. 3, we illustrate the experimental performance of FEC strategies considered in this work. The naive, simple vote repetition coding improves the symbol error rate (SER) but does so rather inefficiently (blue dots). Indeed, the raw received data (green dot) has the SER below the QPSK shot-noise limit (SER ≈8.3% at one photon per bit), but the cumulative energy of repeated symbols grows faster than the observed reduction in SER when compared to the ideal classical receiver. In contrast, the single-shot CAPPs, available from the quantum measurement, significantly improve SER when used for error correction. Therefore, in a head-to-head

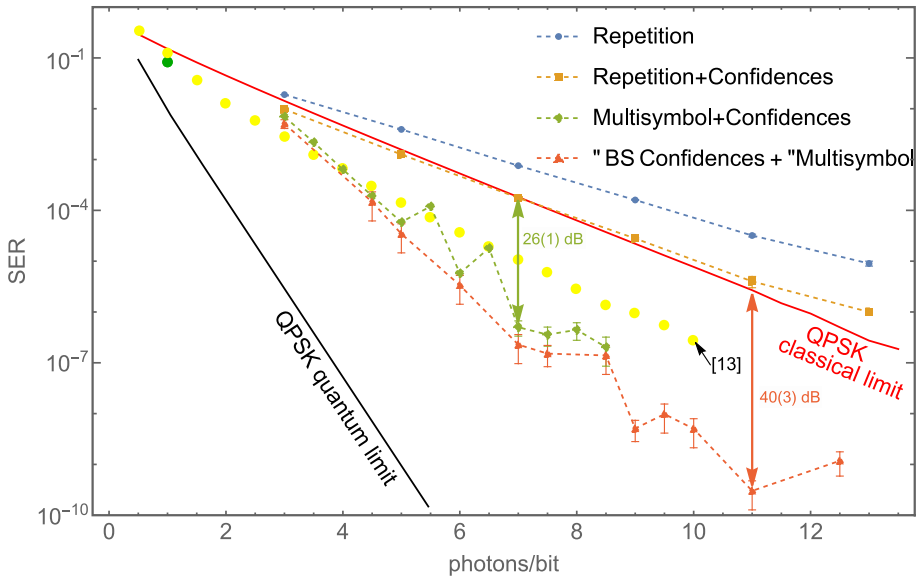

Fig. 3. Reducing symbol error rate using naive and quantum-inspired forward error correction protocols and a comparison to the PNR quantum receiver.[13] Green filled circle shows raw experimental SER. The use of auxiliary symbols in FEC codes results in a higher number of photons required to transmit a bit of information for longer codes, because the auxiliary symbols are redundant from the point of information. Note that best error correction protocols use single-shot accuracies (CAPP vectors) obtained from the quantum measurement. Green diamonds: each QEFEC code used all the experimental data points one time only to construct and test codewords, in this case, the lowest measurable SER is $>10^{-8}$. We demonstrate the SER improvement of 26(1) dB compared to the QPSK classical shot-noise limit, achieved at seven photons per bit. Red triangles: QEFEC codewords constructed by randomly drawing experimental data points until at least three errors occur (labeled as BS for data bootstrapping). The best SER improvement is 40(3) dB below the QPSK classical shot-noise limit, achieved at 11 photons per bit. Yellow points: experimental SER values from Ref. 13. Dashed lines are guides for the eye. Error bars represent one standard deviation calculated as a square root of the number of observed errors.

comparison of decoding the same repetition code, the strategy which uses the maximum cumulative confidence derived from CAPPs provides better performance (orange squares) than the basic "winner takes it all" voting strategy.

B. Quantum measurement advantage using advanced error correction codes

Second, we identify a set of more advanced error correction codes with improved performance. In particular, we build codewords carrying multiple information symbols supplemented with auxiliary symbols. Auxiliary symbols include the result of logical operations, such as bitwise inversion and bitwise XOR, applied to information symbols. Bit values can be assigned in various ways to each of the alphabet states, for example, see the color-coded constellation of QPSK states in the upper left corner of Fig. 4. Other auxiliary symbols used are "physically" distant states (for QPSK, these are states shifted by phase π from the information symbols). An example of the advanced error correction code is presented in Fig. 4. This code uses three information and nine auxiliary symbols. In this example, for QPSK modulation, each information signal can be in one of the four coherent states with phase shifted by $\pi/2$, which corresponds to the total number of valid codewords $4^3 = 64$. To find the energy efficiency of the FEC, notice that each codeword contains $3\log_2 4 = 6$ bits of information and consists of $3 + 9 = 12$ symbols. In the experiment, each symbol corresponds to a coherent optical state with an average energy of two photons (one photon per bit), and therefore the optical power at the receiver remains constant for all the error correction codes considered in this work. However, auxiliary symbols in the codeword are derived from the information symbols and therefore they are redundant and do not add to the number of bits of transmitted information. Thus, codewords in the example consist of 12 symbols, where each symbol is a coherent optical pulse with two photons on average, and the codewords contain 6 bits of information. Therefore, a reduction in the error rate does not come for free with the FEC: the energy consumption of the corresponding QEFEC is four photons/bit (12 symbols $\times$ 2 photons/symbol/6 bits = 4 photons/bit), four times greater than the raw experimental energy consumption for a single symbol.

Here, we test FEC codewords that can be built by adding auxiliary symbols to the information symbols. Auxiliary symbols can be created by repeating and/or combining different bitwise and/or opposite state operations. See the supplementary material for the full list of the multi-symbol QEFEC codes used in this work. The quantum receiver measures and returns the set of CAPPs for each symbol of the received codeword. Then QEFEC algorithm calculates cumulative confidences for each possible codeword by multiplying experimentally obtained CAPPs corresponding to the codewords' symbols. The codeword with the highest confidence is considered a correct message. Each decoded information symbol is compared with the corresponding transmitted information symbol to estimate the SER. As we increase the codewords' length, the SER rapidly decreases, Fig. 3. When we use the experimental data only once to evaluate error correction performance (green diamonds), we obtain a 26 dB improvement over the QPSK classical limit when using QEFEC with seven photons per bit. The overhead associated with each QEFEC code is accounted for in Fig. 3 as the number of photons per bit used by a code. See the supplementary material for photons per bit use of all QEFEC codes shown in Fig. 3. An example of the calculation is given earlier. Note that a further increase in codeword length leads to even higher suppression of errors, so we ran out of experimental data before a single error can be identified. The results with zero errors are not shown in the log scale. Indeed, given the number of experimental measurements of about 10^8, we cannot estimate SERs below 10^{-8} if each measurement result is used only once. To assess the expected error rate of longer codewords, we draw experimental data randomly and allow the use of the same points multiple times; this technique is known as bootstrapping. For this calculation, we require that the algorithm finds at least three errors and calculates SER by dividing the number of errors by the number of received data symbols (red triangles). In comparing a raw SER estimate with the bootstrapping-assisted estimate, we obtain SERs that are similar (to within the uncertainty range); thus, error estimation is not affected by the method used. Our best result is 84(3) dB

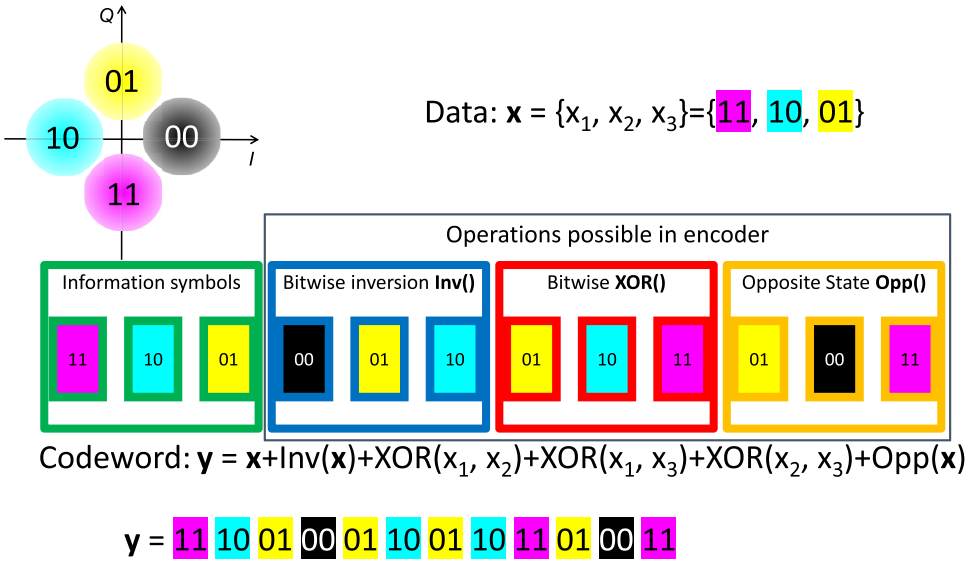

FIG. 4. An example of a multi-symbol quantum forward error correction code with three information symbols using a QPSK communication alphabet. Here, three different operations are used for auxiliary symbols: bitwise inversion, bitwise XOR, and using physically opposite states. Top left inset: a QPSK constellation diagram with color-coding and binary values assigned to different states.

below the initial raw experimental SER, and we end up with just three errors per 10 billion information symbols of user data [see Multisymbol + Confidences (BS) in Fig. 3]! In comparing our results with fundamental bounds and prior work, our result compares favorably to a photon number resolving (PNR) quantum receiver for mesoscopic states of light,[13] and our best result is 40(3) dB lower than the classical homodyne limit for the input states of the same energy. Additionally, we observed no signs of SER saturation with the total optical energy per bit, a typical behavior in quantum receivers.

IV. DISCUSSION

In this report, we experimentally implement quantum-enabled error correction, i.e., where information obtained in the process of quantum measurement enables efficient error-correcting methods. We survey different error correction algorithms and verify that algorithms that use CAPP values (uncertainty estimations extracted from quantum measurement) significantly improve error correction with QEFEC. To put this result in context, this method enables using just 11 optical photons at the receiver to communicate 1 bit of information with the error rate of 3×10^{-9}. Currently, orders of magnitude more photons are required to achieve that level of reliability using state-of-the-art conventional classical receivers. A receiver reported in this work can be immediately employed for practical classical communication when a large optical energy is either not available at the transmitter and/or an optical signal cannot be tolerated by the optical link. For instance, this technique can be applied to quantum networks. In particular, it allows clock synchronization protocols (e.g., via White Rabbit[22,23]) or auxiliary classical channels to share the same fiber with quantum channels without producing any crosstalk. To this end, we estimate that a few orders of magnitude reduction of energy required at the receiver, enabled by quantum measurement, translates to a more than two-fold increase in the maximal link length, especially useful for metropolitan area quantum networks.[24]

To conclude, extra information available in a quantum measurement (single-shot accuracy estimates given by CAPPs) can be practically used to reduce the physical resource (input energy) requirements for reliable communications using any encoding modulation. The most optimal method of using extra information available from the continuous quantum measurement, however, is currently unknown. To this end, there exist capacity-achieving error correction codes such as turbo codes[25] that can be also supplemented with CAPPs; those codes are the subject of future research.

SUPPLEMENTARY MATERIAL

See the supplementary material for the table containing all QEFEC codes tested in the manuscript.

ACKNOWLEDGMENTS

The authors thank Alan L. Migdall and Victor V. Albert for fruitful discussions and proofreading the manuscript.

AUTHOR DECLARATIONS

Conflict of Interest

The authors have no conflicts to disclose.

Author Contributions

Ivan A. Burenkov designed and built the experimental setup, developed computer and FPGA codes, processed and analyzed raw experimental data, developed and assessed quantum-enhanced error correction codes, and led the project. N. Fajar R. Annafianto developed computer and FPGA codes. M.V .Jabir designed and built the experimental setup and collected raw experimental data. A.B. secured partial funding. Sergey V. Polyakov designed the setup, developed measurement protocols, and secured partial funding. The manuscript was written by Ivan A. Burenkov and Sergey V. Polyakov.

Ivan Burenkov: Conceptualization (equal); Data curation (equal); Formal analysis (equal); Software (equal); Supervision (equal); Validation (equal); Visualization (equal); Writing – original draft (equal); Writing – review & editing (equal). **N. Fajar R. Annafianto:** Software (lead). **M. V. Jabir:** Data curation (lead); Methodology (lead). **Abdella Battou:** Funding acquisition (lead). **Sergey V. Polyakov:** Conceptualization (equal); Formal analysis (equal); Resources (equal); Supervision (equal); Writing – original draft (equal); Writing – review & editing (equal).

DATA AVAILABILITY

The data that support the findings of this study and the computer codes developed in this study are available from the corresponding author upon reasonable request.

REFERENCES

[1]C. W. Helstrom, J. Stat. Phys. **1**, 231 (1969).
[2]R. L. Cook, P. J. Martin, and J. M. Geremia, Nature **446**, 774 (2007).
[3]K. Tsujino, D. Fukuda, G. Fujii, S. Inoue, M. Fujiwara, M. Takeoka, and M. Sasaki, Opt. Express **18**, 8107 (2010).
[4]K. Tsujino, D. Fukuda, G. Fujii, S. Inoue, M. Fujiwara, M. Takeoka, and M. Sasaki, Phys. Rev. Lett. **106**, 250503 (2011).
[5]J. Chen, J. L. Habif, Z. Dutton, R. Lazarus, and S. Guha, Nat. Photonics **6**, 374 (2012).
[6]F. Becerra, J. Fan, G. Baumgartner, J. Goldhar, J. Kosloski, and A. Migdall, Nat. Photonics **7**, 147 (2013).
[7]S. Izumi, J. S. Neergaard-Nielsen, S. Miki, H. Terai, and U. L. Andersen, Phys. Rev. Appl. **13**, 054015 (2020).
[8]I. Burenkov, M. Jabir, A. Battou, and S. Polyakov, PRX Quantum **1**, 010308 (2020).
[9]M. V. Jabir, I. A. Burenkov, N. F. R. Annafianto, A. Battou, and S. V. Polyakov, OSA Continuum **3**, 3324 (2020).
[10]M. V. Jabir, N. F. R. Annafianto, I. A. Burenkov, A. Battou, and S. V. Polyakov, npj Quantum Inf. **8**, 63 (2022).
[11]C. Cui, W. Horrocks, S. Hao, S. Guha, N. Peyghambarian, Q. Zhuang, and Z. Zhang, Light: Sci. Appl. **11**, 344 (2022).
[12]I. A. Burenkov, M. V. Jabir, and S. V. Polyakov, AVS Quantum Sci. **3**, 025301 (2021).
[13]F. Becerra, J. Fan, and A. Migdall, Nat. Photonics **9**, 48 (2015).
[14]I. A. Burenkov, N. F. R. Annafianto, M. V. Jabir, M. Wayne, A. Battou, and S. V. Polyakov, Phys. Rev. Lett. **128**, 040404 (2022).
[15]O. Gazi, *Forward Error Correction via Channel Coding* (Springer International Publishing, 2019).
[16]I. A. Burenkov, O. V. Tikhonova, and S. V. Polyakov, Optica **5**, 227 (2018).
[17]F. E. Becerra, J. Fan, G. Baumgartner, S. V. Polyakov, J. Goldhar, J. T. Kosloski, and A. Migdall, Phys. Rev. A **84**, 062324 (2011).
[18]M. Srinivas and E. Davies, Opt. Acta **28**, 981 (1981).
[19]A. Semionov, see https://www.nist.gov/video/quantum-measurement-animated-video for "Quantum measurement animated video."
[20]M. V. Jabir, N. F. R. Annafianto, I. A. Burenkov, M. Dagenais, A. Battou, and S. V. Polyakov, AVS Quantum Sci. **5**, 015001 (2023).

[21]J. Proakis, *Digital Communications*, Electrical Engineering Series (McGraw-Hill, 2001).
[22]M. Lipiński, T. Włostowski, J. Serrano, and P. Alvarez, "White Rabbit: A PTP application for robust sub-nanosecond synchronization," in *IEEE International Symposium on Precision Clock Synchronization for Measurement, Control and Communication* (IEEE, 2011), pp. 25–30.
[23]M. Rizzi, M. Lipinski, P. Ferrari, S. Rinaldi, and A. Flammini, IEEE Trans. Ultrason., Ferroelectr., Freq. Control **65**, 1726 (2018).
[24]I. A. Burenkov, A. Semenova, T. Hala, A. Gerrits, D. Rahnouni, Y.-S. Anand, O. Li-Baboud, A. Slattery, S. V. Battou *et al.*, Opt. Express **31**, 11431 (2023).
[25]C. Berrou, A. Glavieux, and P. Thitimajshima, "Near Shannon limit error-correcting coding and decoding: Turbo-codes. 1," in *Proceedings of ICC'93-IEEE International Conference on Communications* (IEEE, 1993), Vol. 2, pp. 1064–1070.